# Cooperative Assembly of Signal Recognition Particle RNA with Protein SRP19†

Kerfoot P. Walker III, Shaun D. Black, and Christian Zwieb*

*Departments of Molecular Biology and Biochemistry, The University of Texas Health Science Center at Tyler, P.O. Box 2003, Tyler, Texas 75710*

*Received March 30, 1995; Revised Manuscript Received July 17, 1995*®

ABSTRACT: Signal recognition particle (SRP) is a ribonucleoprotein complex involved in the targeting of secretory proteins to the lipid bilayer of the endoplasmic reticulum. SRP contains the protein SRP19, which is an important structural and functional component, believed to promote the assembly of the particle. We have purified the human SRP19 protein to homogeneity from recombinant bacteria which overexpress the polypeptide, and have studied details of the binding to SRP RNA via gel mobility shift and RNase sensitivity assays. SRP19 interacts with two SRP RNA conformers with different affinities such that the more compact RNA species is bound more avidly. Furthermore, binding was found to be highly cooperative. Binding constants and Hill coefficients were determined for several mutant SRP RNAs in which individual RNA helices were deleted. These results confirmed that both SRP RNA helices 6 and 8 are important for SRP19 binding. Enzymatic RNA structure probing of a 150-nucleotide mutant SRP RNA fragment and of the corresponding RNA−SRP19 complex showed that cooperativity may be due to protein-induced conformational changes in the large domain of the SRP RNA. Finally, SRP19 bound specifically not only to SRP RNA but also to the A-form of *Escherichia coli* 5S ribosomal RNA, thereby indicating structural similarities between these two RNA molecules.

Signal recognition particles (SRPs)[1] are present in all organisms (Althoff et al., 1994, Zwieb & Larsen, 1994) and interact with the hydrophobic signal sequences of nascent polypeptides as they emerge from ribosomes during translation (Walter & Lingappa, 1986). This interaction is one of the early steps in the targeting of the SRP−ribosome complex to the SRP receptor (Walter et al., 1984; Wiedmann et al., 1994) and is followed by the cotranslational insertion of microsomal membrane or secretory proteins into the phospholipid bilayer of the endoplasmic reticulum. Particularly well characterized is the mammalian SRP, a stable ribonucleoprotein particle (RNP) composed of a 300-nucleotide RNA molecule (SRP RNA) and 6 polypeptides ranging in size from 9 to 72 kDa (Walter & Blobel, 1983). Protein SRP19 (16 158 kDa) is the only SRP protein that binds to free SRP RNA independently of other SRP components and is therefore believed to be the initiator of SRP assembly (Lingelbach et al., 1988). Furthermore, protein SRP54, which can be cross-linked to the signal peptide (Krieg et al., 1986; Kurzchalia et al., 1986), requires SRP19 to bind (Hann et al., 1992; Römisch et al., 1990; Walter & Blobel, 1983; Zopf et al., 1990). Because SRP19 and SRP54 do not form a heterodimer, binding of SRP54 to SRP RNA appears to be mediated through conformational changes that occur during the formation of the SRP RNA−SRP19 protein complex (Römisch et al., 1990; Zwieb, 1985, 1991b; Zwieb & Ullu, 1986).

Protein SRP19 recognizes not only 3 bp in the distal portion of SRP RNA helix 8 (Zwieb, 1994) but also an RNA tetranucleotide loop (tetraloop) in helix 6 of the SRP RNA (Zwieb, 1992b). Tetraloops occur frequently in RNA molecules, such as the ribosomal RNAs (Gutell et al., 1985; Woese et al., 1990), and have been implicated to interact with primary assembly proteins (Zwieb, 1992a). Consistent with a role of SRP19 in SRP assembly are the multiple contacts identified by systematic site-directed mutagenesis of the protein; more than 40% of the primary structure appears to be necessary for SRP RNA binding (Chittenden et al., 1994; Zwieb, 1991a).

To understand and define further the events that occur during assembly of the SRP, we expressed and purified human SRP19, and used RNA gel mobility shift analyses to study binding of the protein to two conformers of human SRP RNA and to three mutant RNAs with helix truncations (Zwieb, 1991b; Figure 1). Our results demonstrate that binding affinities to the various RNA molecules differ and occur with a considerable degree of cooperativity. By comparing the RNase sensitivities of the free and the complexed RNA molecules we provide experimental evidence that the observed cooperativity may be due to changes in SRP RNA conformation.

## MATERIALS AND METHODS

*Bacterial Expression and Purification of Human Protein SRP19.* An *Nco*I−*Eco*RI restriction fragment containing the

† This work was supported by Grant-in-Aid 93R-556 from the American Heart Association, Texas Affiliate to C. Z.

* Correspondence should be addressed to this author at the Department of Molecular Biology, The University of Texas Health Science Center at Tyler, Highway 271 N., P.O. Box 2003, Tyler, TX 75710. Telephone: (903) 877-7689, (903) 877-7676. Fax: (903) 877-7558. E-mail: zwieb@jason.uthct.edu.

® Abstract published in *Advance ACS Abstracts,* September 1, 1995.

[1] Abbreviations: BSA, bovine serum albumin; dsDNA, double-stranded DNA; DTT, dithiothreitol; *E. coli, Escherichia coli*; LB, Luria−Bertani; EDTA, ethylenediaminetetraacetic acid; HEPES, 4-(2-hydroxyethyl)piperazine-1-ethanesulfonic acid; IPTG, isopropyl β-D-thiogalactopyranoside; PAGE, polyacrylamide gel electrophoresis; RNP, ribonucleoprotein particle; rRNA, ribosomal RNA; tRNA, transfer RNA; SDS, sodium dodecyl sulfate; SRP, signal recognition particle; SRP19, 19 kDa protein of signal recognition particle; SRP54, 54 kDa protein of signal recognition particle; SRP9/14, 9 and 14 kDa proteins of signal recognition particle; SRP68/72, 68 and 72 kDa proteins of signal recognition particle.

0006-2960/95/0434-11989$09.00/0 

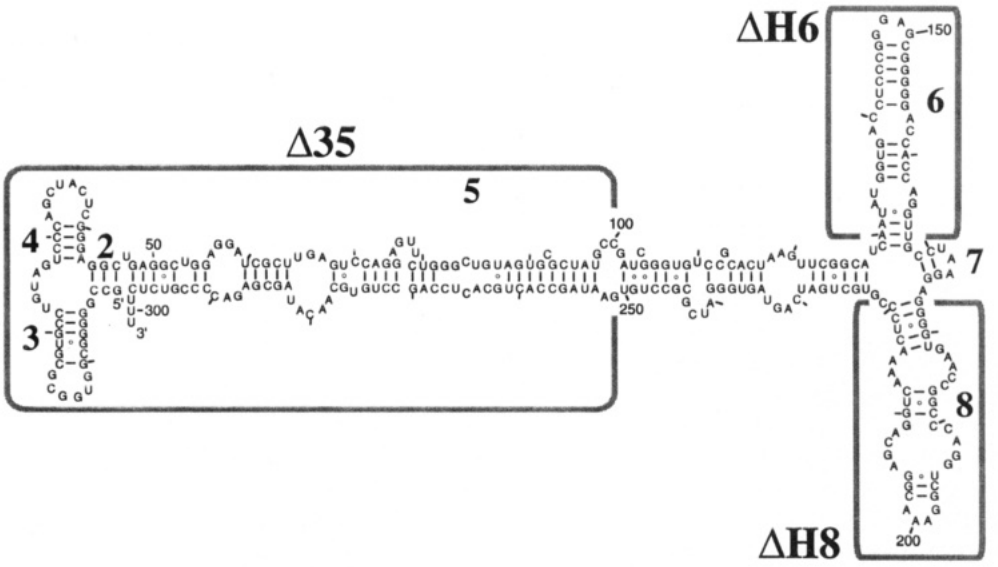


FIGURE 1: Secondary structure of human SRP RNA. Only phylogenetically supported base pairs are shown (Larsen & Zwieb, 1991; Zwieb & Larsen, 1994). Watson−Crick base pairs are connected with a line, and GU interactions are indicated with an open circle. Starting from the 5′-end, SRP RNA helices are numbered from 2 to 8 since helix 1 is only present in the archaebacterial kingdom (Larsen & Zwieb, 1991). Nucleotides are tick-marked in increments of 10 and numbered in increments of 50. RNA portions that are deleted in mutants Δ35, ΔH6, or ΔH8 are indicated by the gray boxes. Details of the secondary structures of these RNAs have been described earlier (Zwieb, 1991b).

human SRP19 gene was isolated from pET19X, a plasmid designed for *in vitro* transcription of SRP19 mRNA by T7 polymerase (Studier et al., 1990; Zwieb, 1991b). This fragment was inserted into *Nco*I−*Eco*RI-restricted plasmid pET-23d (Novagen) using standard cloning procedures (Maniatis et al., 1982). The resulting recombinant plasmid, pET23d-19X, was transformed into competent *E. coli* BL21-DE3 cells (Studier et al., 1990) which were incubated overnight at 37 °C on 10 cm diameter LB agar plates containing 100 μg/mL ampicillin (Sigma). Two 2 L Erlenmeyer flasks, each with 400 mL of LB and 100 μg/mL ampicillin, were inoculated with all colonies from two plates each, and the cultures were grown at 37 °C with vigorous shaking for about 45 min until the $A_{600}$ was between 0.5 and 0.8. Both cultures were used to seed a 20 L fermenter (Bioflo IV, New Brunswick Scientific) containing 11.2 L of LB medium (with enough nutrients for 12 L), 240 mg of ampicillin, 960 mg of methicillin (USB), and 1.2 mL of antifoam 289 (Sigma) kept at 37 °C with aeration. The vessel pressure was 20 psi, and the speed of the stirrer was set to 600 rpm. Expression of SRP19 was induced when the $A_{600}$ of the culture reached 0.8 (after about 2.5 h) by adding IPTG (Gold Biotechnologies) to a final concentration of 1 mM, after which growth was continued for 2 h. Cells were harvested by continuous flow centrifugation at 40 000 rpm in a cooled (4 °C) SK-V4A rotor (in a CEPA, type LE centrifuge) and were kept frozen at −70 °C. The yield was about 2.5 g of wet cells/L of culture.

All subsequent manipulations for protein purification were carried out at 4 °C. Approximately 30 g of frozen cells was resuspended in 150 mL of ice-cold lysis buffer (50 mM Tris-HCl, pH 7.5, 100 mM NaCl, 5 mM DTT, 10% glycerol, and 2 M urea), and 35 mL aliquots of the suspension were passed twice through a French pressure cell (SLM, Aminco) at 15 000 psi. The lysate was submitted to centrifugation for 10 min at 14500*g*. The resulting supernatant was submitted to centrifugation for 4 h at 80000*g*. The supernatant (about 150 mL) was diluted by adding an equal volume of lysis buffer and was loaded onto a Biorex 70 (Bio-Rad) cation exchange column (2.5 cm diameter by 28 cm, total bed volume of about 138 mL) equilibrated in lysis buffer and connected to an FPLC system (Pharmacia). Most *E. coli* proteins appeared in the eluate or were removed from the column with 300 mL of wash buffer at a flow rate of 1 mL/min (50 mM Tris-HCl, pH 7.5, 280 mM NaCl, 5 mM DTT, 10% glycerol, and 2 M urea). The urea was removed slowly, and a buffer change was carried out by applying a linear gradient (300 mL of each buffer at a flow rate of 1 mL/min) from 50 mM Tris-HCl, pH 7.5, 280 mM NaCl, 5 mM DTT, 10 % glycerol, and 2 M urea (wash buffer) to 100 mM $KPO_4$, pH 6.8, 280 mM NaCl, 5 mM DTT, and 10% glycerol (phosphate buffer), after which the column was washed with an additional 100 mL of phosphate buffer. The SRP19 protein was eluted at about 390 mM NaCl in phosphate buffer with a linear gradient from 280 mM to 1 M salt (total gradient volume of 150 mL). Peak fractions, as assessed by SDS−PAGE and staining with Coomassie blue (see below), were pooled, were diluted 5-fold with 100 mM $KPO_4$, pH 6.8, 5 mM DTT, and 10% glycerol, and were loaded (at a flow rate of 0.5 mL/min) onto a heparin−Sepharose (Pharmacia) column (1.6 cm diameter by 12.5 cm, total bed volume about 25 mL) equilibrated in phosphate buffer. The column was washed with 55 mL of phosphate buffer (1 mL/min), and SRP19 was eluted at about 600 mM salt when a NaCl gradient from 280 mM to 1 M in phosphate buffer (total volume 150 mL) was applied. The peak fractions were pooled, and the protein concentration was determined using a modification of the Bradford (Bio-Rad) protein assay (Bradford, 1976); measurements were carried out with 180 μL of the Bio-Rad reagent and 20 μL of sample or BSA standard. The absorbance values at 595 nm were determined with a microtiter plate reader (Vmax, Molecular Devices). In the final purification step, the protein was concentrated by centrifugation to about 65 mg/mL (Amicon Centricon 10, Sorvall RT6000, A500 rotor at 3500*g*), and was loaded onto a Pharmacia Superdex 75 prep grade gel

filtration column (2.6 cm diameter by 60 cm, bed volume about 330 mL) equilibrated in 25 mM Tris-HCl, pH 7.5, 150 mM NaCl, and 5 mM DTT. Peak fractions were pooled and were stored in 50 mM $KPO_4$, 500 mM NaCl, 5 mM DTT, and 50% glycerol, pH 6.8 at −20 °C, until further use. The purity of the preparation was determined by densitometric scanning of the Coomassie blue- and silver-stained gels after SDS−PAGE using an Abaton 300/GS scanner and NIH Image software (Rasband, 1994).

*Gel Mobilities of RNA−Protein Complexes.* Native human SRP RNA and helix-deletion mutant SRP RNAs ΔH6, ΔH8, and Δ35 were synthesized *in vitro* by runoff transcription with T7 RNA polymerase (Stratagene) as described (Zwieb, 1991b). All RNAs were analyzed and quantified on 2% agarose gels with subsequent densitometric scanning (Abaton 300/GS scanner) of the photographs obtained after ethidium bromide staining of gels. RNA samples were extracted with phenol and chloroform, concentrated by ethanol precipitation, and dissolved in small volumes of water. *E. coli* (strain MRE600) 5S ribosomal RNA was obtained from Boehringer.

Binding of purified SRP19 to the various RNAs was carried out in 25 mM Tris-HCl, pH 7.7, 5 mM $MgCl_2$, 100 mM KOAc, 1 mM DTT, and 10% glycerol (SRP19 binding buffer) by gently mixing with the pipet tip in the following order: 1.6 μL of 5-times-concentrated binding buffer, 2 μL of RNA (about 0.2 μg; see Results), 4.4 μL of 25% glycerol, and 2 μL of SRP19 protein diluted in binding buffer to an appropriate concentration (see Results). The samples were incubated at 37 °C for 10 min and were then loaded (without addition of any tracking dye) onto a 6% polyacrylamide gel [acrylamide/bis(acrylamide) ratio of 40/0.8, w/w, 20 mM HEPES, pH 8.3, 0.1 mM EDTA, and 6% glycerol] which had been preelectrophoresed at 15 mA for 30 min with 20 mM HEPES, pH 8.3, 0.1 mM EDTA as a reservoir buffer (Wolffe, 1988). Electrophoresis was continued at 15−20 mA until the bromophenol blue (loaded in a separate slot) had traveled about 15 cm. The gel was stained for 10 min with 1 μg/mL ethidium bromide, and bands on the photographs of the ethidium bromide-stained gels were quantified as described above.

To distinguish complexes with SRP19 from free RNA, gels were fixed and stained with 0.1% Coomassie blue G250 in 40% methanol, 10% acetic acid, for 10 min. The gels were destained with 40% methanol, 10% acetic acid for several hours and then were washed with 50% methanol (reagent grade) overnight, prior to visualization of RNAs (orange−brown color) and complexes (dark gray color) by silver staining (Wray et al., 1981).

Binding parameters were calculated after scanning of the ethidium bromide-stained gels and determination of the free RNA amounts and the amounts present in complexes with protein SRP19 by comparison with known amounts of *E. coli* 5S ribosomal RNA. A sigmoidal function, $y = 100/[1 + (a/x)^b]$, where $y$ is the percent of complex formed at a given protein SRP19 concentration $x$, $a$ is the dissociation constant ($K_d$), and $b$ is the Hill coefficient, was fitted to the experimental data with the program MCF (Raner, 1993). Binding data could not be fit to a simple equilibrium model.

*Sensitivity of RNA−Protein Complexes to RNases.* The 3′-ends of Δ35 or 5S rRNA were labeled with cytidine 3′,5′-[5′-$^{32}$P]bis(phosphate (Amersham) using T4 RNA ligase (New England Biolabs) and the vendor-supplied conditions, but with incubation at 4 °C overnight as described (Zwieb, 1985). RNAs were extracted with phenol, phenol/chloroform, and chloroform; 3 M sodium acetate (pH 6) was added to the sample to a final concentration of 300 mM, and the RNAs were precipitated with 3 volumes of ethanol and incubated at −70 °C for 20 min. RNAs were concentrated by centrifugation, washed once with 80% ethanol, dried, and were dissolved in a small volume of Tris−borate, EDTA containing 5 M urea for purification on a 1 mm thick 6% polyacrylamide−urea gel as used for DNA sequencing (Maniatis et al., 1982). The migration positions of the intact RNAs were localized by a brief autoradiography. RNA-containing slices were cut from the gel and extracted by incubation at room temperature in 300 μL of 500 mM ammonium acetate, 10 mM EDTA, and 0.2% SDS, for 4 h with occasional shaking. The gel slices were removed, and 3 volumes of ethanol were added to the sample. RNAs were concentrated and washed with three ethanol precipitations before they were dissolved in 20 μL of water.

RNA gel shift experiments with the radiolabeled Δ35 RNA were carried out as described above using SRP19 concentrations that yielded about equimolar amounts of free and bound RNA. After autoradiography, gel strips of about 20 mm by 2 mm were cut from the first-dimension lane. They were incubated for 30 min at 37 °C and submerged in 1 mL of SRP19 binding buffer (see above) containing 0.05% bromophenol blue and 0.05% xylene cyanol (to stain the strips) and with either 0, 1 unit, or 5 units of RNase T1 (Calbiochem), or with 1, or 3 ng of RNase A (Boehringer). The gels were washed once with 1 mL of SRP19 binding buffer for 5 min at room temperature and once with 1 mL of ice-cold Tris−borate, EDTA buffer for 2 min and were loaded onto a 1 mm thick 12% polyacrylamide−urea gel. Electrophoresis was in Tris−borate, EDTA buffer at 80 W until the bromophenol blue dye had migrated about 37 cm. The gel was removed from the glass plates, covered with Parafilm, and exposed to X-ray film.

Mobilities of the radioactive spots on the two-dimensional gels were assigned to nucleotide positions of the respective RNAs by partial digestion of the 3′-end-labeled Δ35 RNA and 5S RNAs with RNase A (for cytosine and uracil) or RNase T1 (for guanine) after electrophoresis of the products on 12% polyacrylamide−urea gels in Tris−borate, EDTA. Each 6 μL RNA sequencing reaction contained 5 μg of carrier tRNA (from calf liver, Boehringer) and about $10^4$ cpm of $^{32}$P-labeled RNA. RNase T1 digestions were carried out in 4 M urea, 0.5 mM EDTA, and 10 mM sodium citrate, pH 3.5, with 0.003 unit of enzyme (Calbiochem); incubation was at 50 °C for 15 min. RNase A digestions were in 4 M urea, 0.5 mM EDTA, and 10 mM Tris-HCl, pH 7.5, with 1 ng of RNase A (Boehringer) per reaction and incubation at 50 °C for 15 min. A sequencing ladder was produced by acid hydrolysis of the respective RNAs in 4 M urea, 110 mM $H_2SO_4$, with incubation for 15 s in a boiling water bath followed by neutralization with 2 μL of 1 N NaOH. All sequence reactions received 50 μL of Tris−EDTA, 6 μL of 3 M sodium acetate (pH 6), and 180 μL of ethanol prior to incubation at −70 °C to precipitate the RNAs. After centrifugation, the pellets were washed once with 80% ethanol, dried, and dissolved in a small volume of loading buffer containing 4 M urea, bromophenol blue, and xylene cyanol. Aliquots of the samples were loaded on a 12% polyacrylamide−urea gel in two sets separated by a 2 h time interval. Electrophoresis proceeded until xylene cyanol had

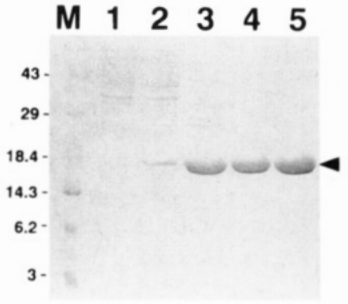


FIGURE 2: Purification of human SRP19. Proteins were separated on a 15% polyacrylamide−SDS gel and stained with Coomassie blue G250. Lane 1, protein extract from uninduced *E. coli* cells; lane 2, protein extract from *E. coli* cells induced with IPTG for 2 h; lane 3, pooled eluate after Biorex 70 chromatography; lane 4, pooled eluate after chromatography on heparin−Sepharose; lane 5, pooled eluate from chromatography on Superdex 75; M, low molecular mass markers (BRL) with protein sizes in kilodaltons.

traveled 12 cm and 24 cm, respectively. The known 5S rRNA and Δ35 RNA sequences (Erdmann et al., 1985; Zwieb, 1991b) were recognized in the autoradiogram and compared to the mobilities of RNA fragments on the two-dimensional polyacrylamide gels.

## RESULTS

*Purification of Human SRP19.* The human SRP19 gene (Lingelbach et al., 1988) was cloned under T7 promoter control of vector pET23d (Novagen) and was confirmed by sequencing of the DNA with Sequenase version 2 (United States Biochemicals). To increase expression yields, we used only freshly transformed competent *E. coli* BL21-DE3 cells as described under Materials and Methods. After induction of SRP19 synthesis by IPTG and analysis of the culture via SDS−PAGE, SRP19 constituted about 30% of the total cellular protein content (Figure 2). The majority of the SRP19 was insoluble in lysis buffers without urea, whereas 5 M urea was sufficient to solubilize the protein completely (data not shown). About two-thirds of the protein remained in the pellet of the high-speed centrifugation at the 2 M urea concentration employed (Materials and Methods), which was expected to keep the solubilized SRP19 in a partially-folded state. Furthermore, using the lower urea concentration reduced the amount of contaminating proteins that would otherwise appear in the subsequent purification steps. After the slow and gradual removal of the urea from the Biorex-bound SRP19, we confirmed the activity of the protein in RNA gel mobility shift assays with *in vitro*-transcribed Δ35 RNA (see Materials and Methods). Typically, the protein was about 70% pure after elution from the Biorex 70 column, about 90% pure after chromatography on heparin-Sepharose, and more than 99% pure after Superdex 75 gel filtration (Figure 2). We routinely obtained about 10 mg of active pure protein from 30 g of cells.

*Interaction of Protein SRP19 with RNA.* We studied the formation of SRP19 complexes with SRP RNA, Δ35 RNA, two helix-deletion mutants (ΔH6 and ΔH8, Figures 1 and 3), and 5S ribosomal RNA (Figure 4) in gel mobility shift assays (Wolffe, 1988; Zwieb & Brown, 1990). This approach allowed us to distinguish between the various RNA conformers present under nondenaturing conditions (Zwieb, 1985; Zwieb & Ullu, 1986). The conformers were thermodynamically stable not only in the polyacrylamide gel matrix but also in solution. This was determined by separating and extracting the various RNAs from the gel, incubating for several hours under protein binding conditions (see Materials and Methods), and analysis by nondenaturing gel electrophoresis. The A- and B-conformers showed no signs of equilibration/interconversion in this experiment. Purified SRP19 was combined with various *in vitro* transcribed RNAs as described under Materials and Methods, and unbound RNAs and complexes were separated on nondenaturing polyacrylamide gels. The mobilities of the RNAs relative

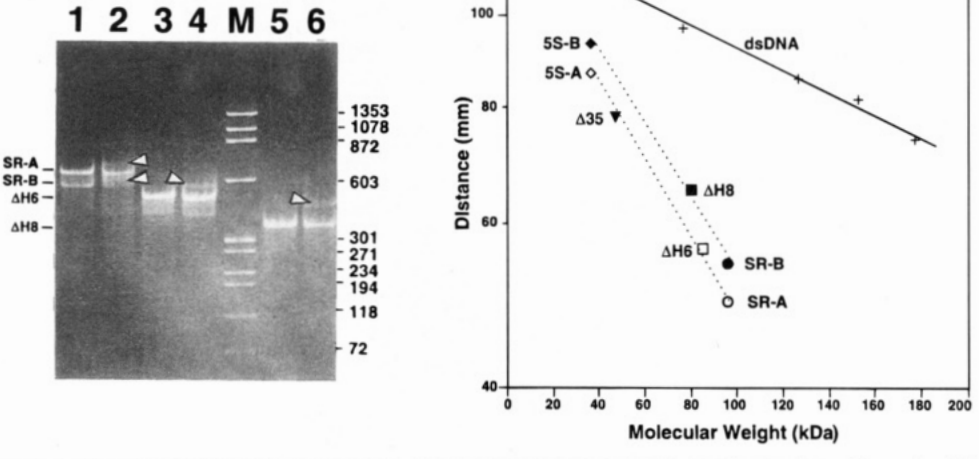


FIGURE 3: Mobilities of SRP RNAs and SRP19 complexes. After electrophoresis on 6% nondenaturing polyacrylamide gels, RNAs were stained with ethidium bromide (left panel). Lane 1, SRP RNA, no SRP19; lane 2, SRP RNA, with SRP19; lane 3, ΔH6 RNA, no SRP19; lane 4, ΔH6 RNA, with SRP19; lane 5, ΔH8 RNA, no SRP19; lane 6, ΔH8 RNA, with SRP19; M, dsDNA molecular mass markers with the number of base pairs marked next to lane 6. The mobilities of the A-form of SRP RNA (SR-A), the B-form of SRP RNA (SR-B), and the mutant RNAs ΔH6 and ΔH8 are indicated next to lane 1. The arrowheads point to RNA−protein complexes as identified by silver staining (see Materials and Methods). The graph on the right shows mobilities for the two SRP RNA conformers (SR-A, SR-B), several mutant derivatives (ΔH6, ΔH8, and Δ35), and the A- and B-conformers of *E. coli* ribosomal RNA (5S-A and 5S-B), relative to the mobilities of double-stranded DNA fragments from *Hae*III-digested φX174 DNA (dsDNA). 5S-A, A-conformer of *E. coli* 5S rRNA (◇); 5S-B, B-conformer of *E. coli* 5S rRNA (◆); Δ35, helix-deletion mutant missing the small SRP RNA domain (▼); ΔH6, deletion of helix 6 of SRP RNA (□); ΔH8, deletion of helix 6 of SRP RNA (■); SR-A, A-conformer of SRP RNA (○); SR-B, B-conformer of SRP RNA (●).

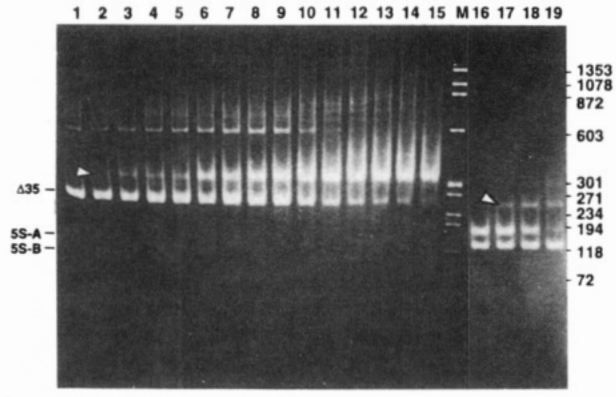


FIGURE 4: Electrophoresis of RNAs and complexes with SRP19 on 6% nondenaturing polyacrylamide gels. Lanes 1−15 contain 160 ng of Δ35 RNA and various concentrations of protein SRP19 from 16 ng (lane 2) to 336 ng (lane 15). Lanes 16−19 contain 400 ng of 5S rRNA with 24 ng (lane 17), 48 ng (lane 18), and 96 ng of SRP19 (lane 19). M: dsDNA molecular mass markers from *Hae*III-digested φX174 DNA with the number of base pairs marked next to lane 19. The arrowheads point to RNA−protein complexes identified by silver staining (see Materials and Methods).

to dsDNA were measured after staining with ethidium bromide. Figure 3 shows that substantial amounts of both a slow-moving SRP RNA conformer (SR-A) and a faster-moving conformer (SR-B) were formed. In contrast, the ΔH6 RNA existed predominantly as a relatively slow-moving component (lane 3); the ΔH8 RNA appeared exclusively as a conformer that migrated relatively fast (lane 5). The graph in Figure 3 shows that the mobility of the Δ35 RNA conformer corresponded to the slow-moving conformers of SRP RNA (SR-A) and of 5S rRNA (5S-A). An RNA species that may represent Δ35 RNA dimers was present in only minor amounts (Figure 4). All RNAs migrated considerably slower than double-stranded DNA fragments of the same molecular weight (Figure 3).

We distinguished RNA−protein complexes from the unbound RNAs by staining the native gels with Coomassie blue and silver (Materials and Methods), such that complexes appeared as dark gray bands (marked with arrowheads in Figures 3 and 4) and the free RNAs displayed a brown or orange color. All RNAs, with the exception of the B-form of *E. coli* ribosomal RNA (Figure 4, lanes 16−19), bound protein SRP19 to some degree; however, the relative amount of complex formed was quite variable. These results indicated different affinities of SRP19 not only to the various mutant RNAs but also to the various SRP RNA and 5 S RNA conformers. For example, binding to the SR-B RNA was more pronounced than to the SR-A RNA or to any of the SRP RNA mutant derivatives (Figure 3).

To determine the SRP19 binding constants, variable protein concentrations were used in gel shift mobility experiments with the SRP RNA or its mutant derivatives. After electrophoresis, gels were stained with ethidium bromide and photographed, and the photographs were scanned to determine the intensities of the bands (Rasband, 1994). With every experiment, a standard curve with known amounts of 5S rRNA was produced to assure linearity of the response ($R^2 > 0.99$). An example of this analysis with the Δ35 RNA is shown in Figure 4 (lanes 1−15). Multiple protein-containing bands appeared at high protein/RNA ratios, which is consistent with the tendency of the RNA to form complexes with more than one protein molecule.

Table 1: Binding Characteristics of Protein SRP19 with the Various RNAs and Their Conformers As Determined by Gel Shift[a]

| RNA | midpoint $K_d$ (μM) | Hill coefficient |
|---|---|---|
| SR-A | 0.29 ± 0.04 | 2.1 ± 0.3 |
| SR-B | 0.079 ± 0.01 | 1.6 ± 0.4 |
| ΔH6 | 0.49 ± 0.01 | 2.5 ± 0.1 |
| ΔH8 | 0.40 ± 0.05 | 3.3 ± 1.1 |
| Δ35 | 0.23 ± 0.02 | 1.4 ± 0.1 |
| 5S-A | 0.28 ± 0.04 | 6.0 ± 0.1 |

[a] Numbers were derived from at least two independent experiments and indicate the $K_d$s at the midpoint of the sigmoidal binding curve and the standard deviations with corresponding Hill coefficients.

Because of this nature of the binding interaction, we determined the degree of complex formation by measuring the amount of RNA that remained unbound at variable protein concentrations. The absolute amount of RNA in the binding assay was calculated from a standard curve with known amounts of 5S rRNA separated on the same gel. A sigmoidal curve was fitted to the data (Materials and Methods), and midpoint dissociation constants ($K_d$) and Hill coefficients were calculated for SR-A, SR-B, ΔH6, ΔH8, Δ35, and 5S-A. Table 1 shows that the greatest affinity of protein SRP19 was for the high-mobility form of the SRP RNA (SR-B). We determined that the binding of SRP19 to SR-A, Δ35, or 5S-A was about 3−4 times weaker than binding to SR-B, whereas the affinity of SRP19 to the helix-deletion mutants ΔH6 and ΔH8 was reduced by a factor of 5−6. Indications of weak binding of SRP19 to 5S-B were observed only at a more than 5-fold molar excess of the protein. Nonetheless, under the assay conditions, SRP19 bound only to SRP RNA (or the respective mutant RNAs) and 5S-A, but not to tRNA or linear, circular, or supercoiled DNA.

All RNAs that bound SRP19 specifically demonstrated a significant deviation from classical binding equilibria as indicated by the Hill coefficient (Table 1). The deviation was most pronounced with the A-form of the 5S rRNA (5S-A), followed, in decreasing order, by the ΔH8, ΔH6, SR-A, SR-B, and Δ35 RNAs, but each of those exhibited considerable positive cooperativity upon binding with SRP19. These results indicated the possibility that upon binding of protein SRP19 conformational changes occurred in the RNA or in the protein. This idea was supported further by the finding that SRP RNA and 5S rRNA existed in a variety of conformers and that binding affinities depended on the conformational state (Table 1). Cooperative binding of SRP19 to the Δ35 RNA was detected also by monitoring fluorescence quenching of the single tryptophan at position 72 (data not shown). However, complex fluorescence changes in the sample that occurred upon titration with RNA prevented us from determining the saturation point unambiguously.

*RNase Sensitivities of RNA Conformers and RNA−SRP19 Complexes.* To explore the possibility that conformational changes were induced in the SRP RNA by its interaction with protein SRP19, we determined the RNase sensitivities of *E. coli* 5S rRNA and compared it with the sensitivities of the free Δ35 RNA and the Δ35 RNA−SRP19 complex. We chose these two RNAs because their sizes (120 and 151 nucleotides, respectively) and secondary structures are similar (Figure 6). Secondly, a comparable degree of folding of the 5S-A conformer and the Δ35 RNA was indicated not only

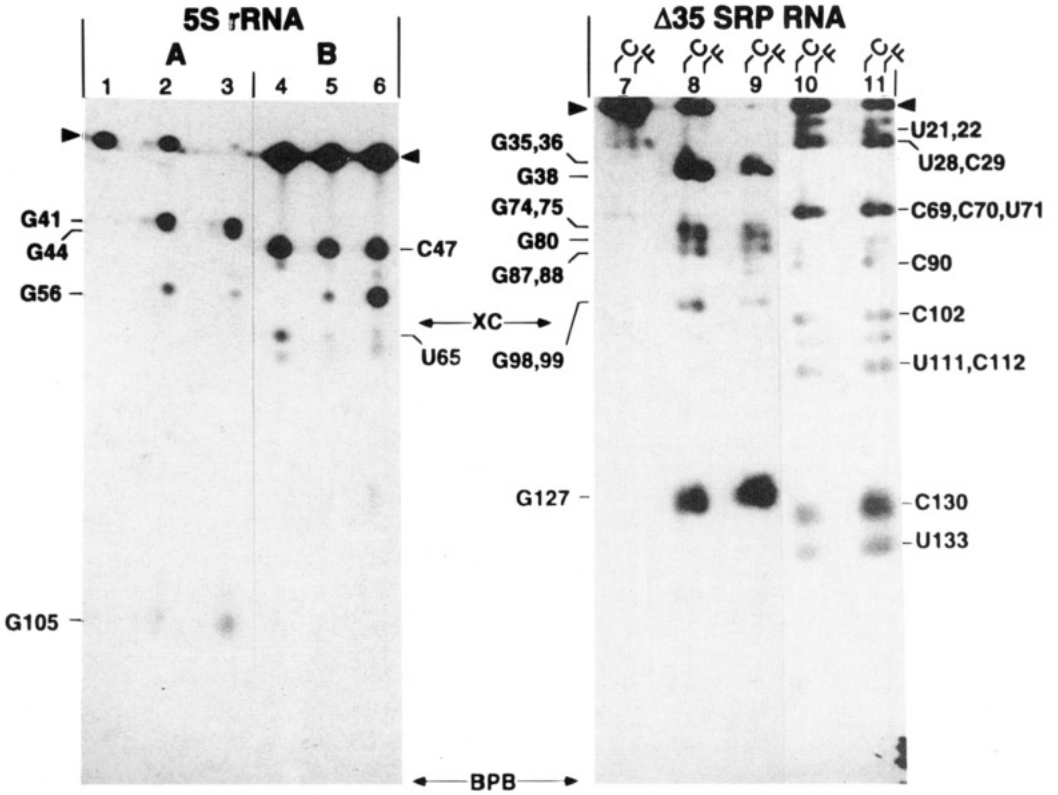


FIGURE 5: Autoradiogram of 5S rRNA conformers, Δ35 RNA, and Δ35 RNA−protein complexes, partially digested with RNases after separation in the first dimension of electrophoresis. Migration was from left to right on a nondenaturing 6% polyacrylamide gel in the first dimension. Gel slices were then treated mildly with RNases, and RNAs were separated in the second dimension (electrophoresis from top to bottom) on denaturing 12% polyacrylamide gels. Left panel: partial digestion of *E. coli* 5S rRNA: lane 1, undigested A-form; lane 2, 5S-A digested with 1 unit of RNase T1; lane 3, 5S-A digested with 5 units of RNase T1; lane 4, undigested B-form; lane 5, 5S-B digested with 1 unit of RNase T1; lane 6, 5S-B digested with 5 units of RNase T1. Right panel: partial digestion of free Δ35 RNA (F) and Δ35 RNA−SRP19 complexes (C): lane 7, undigested; lane 8, digested with 1 unit of RNase T1; lane 9, digested with 5 units of RNase T1; lane 10, digested with 1 ng of RNase A; lane 11, digested with 3 ng of RNase A. Arrowheads indicate the position of the undigested RNAs. Numbers refer to nucleotide positions of RNase-sensitive sites; RNase T1-accessible sites are shown on the left side and RNase A-accessible sites are shown on the right side of each panel. The arrows labeled XC and BPB mark the positions of xylene cyanol and bromophenol blue, respectively.

by structural comparison but also by their relatively equivalent mobilities on native gels (Figure 3). Thirdly, SRP19 was shown to be present only in the large domain of the SRP (Gundelfinger et al., 1983); this fragment corresponds to the Δ35 RNA (Zwieb, 1991b). Lastly, by deleting the 3′- and 5′-ends of the RNA, we confined the binding, thereby avoiding potential secondary effects caused by an interaction of the two SRP domains (Selinger et al., 1994). The 3′-ends of *E. coli* 5S rRNA and of *in vitro* transcribed Δ35 RNA were labeled with $^{32}P$. RNA molecules were first purified by gel electrophoresis and were then incubated under SRP19 binding conditions as described under Materials and Methods. The samples were analyzed by two-dimensional gel electrophoresis which included a limited digestion of the RNA within the gel after electrophoresis in the first dimension. This allowed us to detect differences in the RNase sensitivities not only between the various conformers but also between the free and the complexed RNAs using uniform conditions. The specific positions of RNA hydrolysis were identified in sequencing reactions carried out in parallel with aliquots of the end-labeled RNAs (Materials and Methods).

The left panel of Figure 5 shows that, under identical RNase treatment conditions, the 5S-A conformer was more readily digested with RNase T1 (lanes 2 and 3) than was the 5S-B conformer (lanes 5 and 6). In agreement with earlier findings (Douthwaite & Garrett, 1981), the guanine residues at positions 41, 44, and 105 were easily attacked by RNase T1 when the 5S RNA was in the A-form. They were, in contrast, inaccessible to the enzyme when present in the B-conformation, indicating that 5S-B was folded more tightly than 5S-A; this interpretation is also consistent with the electrophoretic mobilities of the two 5S RNA conformers (see Figure 4 and Discussion). Although the cytosine at position 47 became hypersensitive toward spuriously present RNases only in the 5S-B RNA (lanes 4−6), most of 5S-B remained undigested even at high RNase T1 concentrations.

To determine RNase sensitivities in the Δ35 RNA complex with protein SRP19, we mixed purified end-labeled Δ35 RNA and SRP19 under conditions that yielded about equimolar amounts of free and protein-bound RNA. Since the RNA−protein complex was stable when separated from the free RNA and the free protein by electrophoresis on nondenaturing gels, we were able to probe the structure of the complex directly in gel slices. After separation in the first dimension, free and complexed RNAs in the gel slices were digested with RNase T1 or RNase A under equivalent conditions, and the digestion products were analyzed on denaturing second-dimension gels as described under Materials and Methods. Figure 5 (lanes 2, 3, 8, and 9) shows that the Δ35 RNA was about as vulnerable to RNase digestion as the 5S-A conformer. Somewhat surprisingly, the Δ35

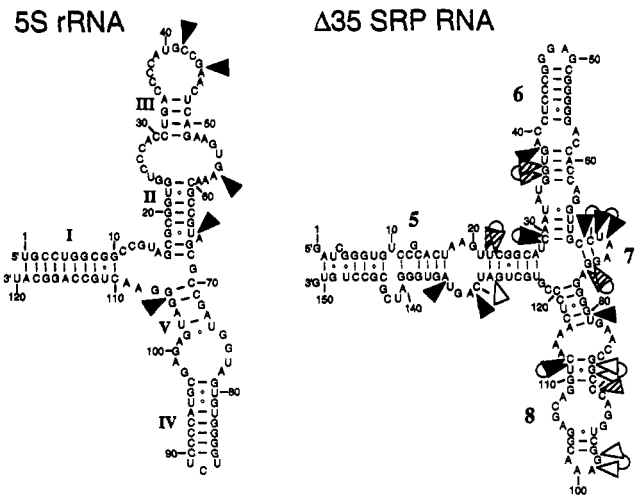


FIGURE 6: Secondary structures of *E. coli* 5S ribosomal RNA (Fox & Woese, 1975) and Δ35 RNA (Zwieb, 1991b). Small numbers indicated nucleotide positions. Roman numerals mark helices in 5S rRNA (Fox & Woese, 1975). Large numbers 2−8 are for the seven helices according to the nomenclature by Larsen and Zwieb (1991). Solid arrowheads mark sites in 5S rRNA and Δ35 RNA that are accessible to RNase T1 or RNase A; open arrowheads indicate sites that are less accessible when protein SRP19 is bound; and hatched arrowheads indicate sites with enhanced RNase sensitivity in the Δ35 RNA−SRP19 complex. Connected arrowheads indicate ambiguities between the assigned cutting sites.

RNA and the Δ35 RNA−SRP19 complex were about equally sensitive toward digestion by both RNase T1 (lanes 8 and 9) and RNase A (lanes 10 and 11) as indicated by the amount of undigested Δ35 RNA (marked by arrows) that remained in lanes labeled free (F) and complexed (C).

As in 5S rRNA, only a limited number of nucleotides of the Δ35 RNA were accessible to the RNases under the mild RNA digestion conditions employed. RNA sequencing revealed that cleavages occurred preferably at nucleotide positions 28, 29, 38, 69−71, and 127. Minor cuts, representing either secluded sites or secondary cleavages, occurred at positions 74, 75, 80, 87, 88, 90, 98, 99, 102, 111, 112, 130, and 133. Figure 6 shows the positions of these RNase-sensitive nucleotides in the predicted secondary structure of the Δ35 RNA (Larsen & Zwieb, 1991; Zwieb & Larsen, 1994).

Although overall both the free (F) and the complexed (C) Δ35 RNAs were about equally sensitive toward RNase digestion, RNA structure probing identified several important differences in sites that were accessible or protected: nucleotides at positions 87, 88, 98, and 99 were somewhat protected in the complex; in contrast, nucleotides at positions 21, 22, 35, 36, 74, and 75 were more accessible when SRP19 was bound, whereas the nucleotides at positions 21, 22, 35, 36, and 90 became RNase-sensitive in the complex only.

## DISCUSSION

*Purification of Human SRP19.* The overexpressed recombinant human SRP19 was purified by chromatography on Biorex, heparin, and Superdex stationary phases. In the early stages of the purification, 2 M urea was present to solubilize SRP19 and to prevent its association with bacterial proteins. Although SRP19 was not completely recovered at this urea concentration, certain contaminating bacterial proteins that became soluble only in 5 M urea were thus removed early in the preparation (Materials and Methods). To restore the activity of the protein, the urea was gradually removed while SRP19 remained bound to the Biorex column. This reconstitution was possible even when samples were prepared in 5 M urea; however, a slow and gradual removal of the denaturant was important for regaining the RNA binding activity (data not shown).

In earlier studies, unknown amounts of radioactively-labeled protein were translated in a cell-free system (Lingelbach et al., 1988; Zwieb, 1991a,b), which made it impossible to determine binding constants and details of the binding interaction. In these, RNA was in large excess, and various proteins from the wheat germ translation system were present at unknown stoichiometric concentrations; protein SRP19 bound equally well to native SRP RNA and to a mutant derivative, the Δ35 RNA (Zwieb, 1991b). The latter mutant corresponds to the large domain of the SRP (Figure 1). In contrast, with purified components, we determined that binding is significantly weaker to the Δ35 RNA than to SRP RNA (Table 1). This result may indicate communication between the small and large domains of the SRP, such that RNA sequences from the small domain (helices 2−4 and a portion of helix 5) facilitate binding of SRP19. Consistent with this finding, genetic and biochemical evidence for direct or indirect interactions between the small and large domains has been provided recently for a fungal SRP homolog (Selinger et al., 1994).

*Mobilities of RNA Conformers.* Conformational differences in the various RNAs were detected by their variable mobilities in nondenaturing polyacrylamide gels. Reduced mobilities usually reflect deviations from straight rods, as has been demonstrated in the study of DNA bends (Wu & Crothers, 1986; Zwieb et al., 1989). Curved or bent RNAs, and RNA molecules containing loops and bulges, also migrate slower when compared to an unbent molecule of the same molecular weight (Gast et al., 1994; Tang & Draper, 1994). Similarly, a molecule that either is branched or contains internal loops as a result of a cross-link migrates considerably slower than its linear equivalent when the structural differences are exposed under denaturing electrophoresis conditions (Zwieb & Brimacombe, 1980; Zwieb & Schüler, 1989). Since both the SRP RNA and the 5S rRNA are branched and contain numerous helices and internal loops (Figures 1 and 6), we expected that they would migrate slower than straight DNA molecules of the same molecular weight (Figure 3).

Although the mobility differences between the A- and B-conformers of the SRP RNA and of the 5S rRNA are difficult to explain without a precise knowledge of the three-dimensional structure, we postulate that the faster-moving B-conformers are more compact. This assertion is supported experimentally by the increased resistance of 5S-B toward RNase T1 digestion (Figure 5). Another factor known to increase the electrophoretic mobility is a decrease in flexibility of the molecule (Gast & Hagerman, 1991). Therefore, the slower-moving A-forms of 5S rRNA and SRP RNA not only may be more loosely structured than their corresponding B-forms but also may be more flexible.

*SRP19 Binding to Various SRP RNA Conformers.* Binding of SRP19 was most effective to the SR-B form, which we considered to be more compact and/or less flexible than the SR-A conformer. The $K_a$ ($1.26 \times 10^7$ $M^{-1}$) of SR-A was about 3.5 times higher than that of SR-B, and almost 1 order of magnitude higher than that for the binding of L18 to 5S

RNA [$1.5 \times 10^6$ $M^{-1}$ (Christensen et al., 1985)], thereby confirming SRP19's strong affinity to SRP RNA in the absence of any other factors. By site-directed mutagenesis, we demonstrated earlier the tight association of the protein with the SRP RNA and showed that at least two sites on the RNA (helix 6 and helix 8) (Zwieb, 1992b, 1993) and five sites on the protein encompassing more than 40% of the primary structure were involved (Chittenden et al., 1994). It is conceivable that the SRP-B conformation accommodates SRP19 such that a larger number of interactions can take place. Furthermore, the interaction with helix-deletion mutants ΔH6 and ΔH8 was impaired, thereby confirming that both helixes are part of the SRP19 binding site (Zwieb, 1991b). One explanation for the weaker binding to the SRP-A conformer may be that the angle between helices 6 and 8 has widened such that fewer RNA−protein interactions are possible; however, a more detailed knowledge of the structure of the large SRP domain will be required before the assembly of SRP19 can be fully understood.

SRP19 bound to Δ35 RNA about as well as to SR-A, which is consistent with the conformational state of these two molecules as judged by their electrophoretic behavior (Figure 3). In a binding assay with a multitude of components that is expected to contain a substantial amount of the SR-A conformer, the overall binding to SRP RNA and Δ35 RNA was about equally effective (Zwieb, 1991b). A comparison of these earlier findings with the new data obtained in a purified system may indicate that previously the SRP RNA was in fact not in the A-conformation. It is possible that components present in wheat germ lysates, such as certain plant SRP proteins (Zwieb, unpublished), selectively impaired binding to SR-A. It also cannot be excluded that the *in vitro* translated SRP19 had lost certain binding determinants which were intact in the recombinant purified protein.

*Cooperative Binding of SRP19 to SRP RNA.* The significant deviation from classical binding curves can be best explained by conformational changes that occur in the RNA upon protein binding. There are, however, other explanations that may contribute to an increased Hill coefficient. Cooperative binding may reflect the ability of SRP19 to dissociate RNA dimers, as we have observed experimentally in the case of Δ35 RNA (Figure 4). Furthermore, changes in protein conformation may contribute significantly to the binding interaction. Also, the possibility exists that more than one SRP19 molecule may interact with the SRP RNA in the early stages of the assembly process. Although the analysis of RNase-sensitive sites in the complex and the free RNA provides experimental evidence for conformational changes to occur in the RNA, the relative contribution to the overall effect on cooperativity was not determined.

Analyzing the RNase sensitivities of the free and complexed Δ35 RNA showed that both were about equally susceptible. The overall sensitivity remained similar, because there appeared to exist a balance between sites that were protected and sites that became accessible in the complex. All sites were located throughout helices 5, 6, 7, and 8, which argues that SRP19 is crucial to the organization of the large SRP domain; this finding is consistent with earlier proposed models (Chittenden et al., 1994; Zwieb, 1989, 1992b, 1993, 1994). Detailed systematic site-directed mutagenesis showed that the helix 6 tetraloop (positions 147−150) is an important part of the SRP19 binding site. This loop is extremely resistant to RNase digestion even in 4 M urea at 50 °C (not shown); therefore, we were unable to demonstrate protection of the tetraloop of helix 6 by SRP19.

*Implications for SRP Assembly and Function.* Because the helix 6 tetraloop is of considerable stability and contains, at the third position, a phylogenetically conserved adenosine which is essential for binding, we speculate that it serves as a nucleation site in the first steps of SRP assembly. A function of SRP19 might be to initiate assembly at the tetraloop and subsequently to assure proper organization of the remaining RNA of the large SRP domain using interactions in helix 6 and helix 8. Evidence from experiments in which mammalian SRP54 bound to *E. coli* 4.5S RNA (Ribes et al., 1990; Zopf et al., 1990) indicates that helix 8 is the primary binding site for the M-domain of protein SRP54. Furthermore, it was shown that the *Mycoplasma mycoides* SRP54 homolog protects helix 8 from digestion by RNase A (Samuelsson, 1992). The protection and the enhancement we detect in helix 8 upon binding of SRP19 show that SRP19 is indeed involved in the organization of the SRP54 binding site and explain how SRP19 promotes binding of SRP54 during SRP assembly. We do not exclude possible secondary protein−protein contacts between SRP19 and SRP54 that may occur during the later stages of the assembly process.

Another important role of SRP19 may be to facilitate the movement of SRP through the SRP cycle. Cross-linking experiments demonstrate that free SRP54 interacts with the signal peptide (Krieg et al., 1986; Kurzchalia et al., 1986), indicating that SRP54 may dissociate from the SRP when binding to the signal. It is conceivable that a SRP19-mediated conformational change in SRP RNA could regulate the association of SRP54 with SRP RNA and thereby influence GTP-dependent release of signal sequences (Miller et al., 1993).

*Binding of SRP19 to 5S rRNA.* Similarities between 5S rRNA and SRP RNA on the sequence level have been described (Boehm, 1987; Zwieb, 1985). However, when primary structures of SRP RNAs from additional species became available (Zwieb & Larsen, 1994), the phylogenetically-conserved character of these sequences was not confirmed in all species. There remains, however, an overall similarity in topology of the RNAs on the secondary structure level (Figure 6), which is defined by a junction of three or four helices at their proximal parts. SRP19 bound only to the A-form of the 5S rRNA which is most likely characterized by a conformation that is more openly structured than the B-form. The remarkably high Hill coefficient of the SRP19 binding reaction with the 5S-A RNA indicates that this conformer not only may be more loosely structured but also may be quite flexible. It is possible that, because of this added flexibility, 5S-A mimics an SRP19 binding site which may include a GNAR-tetraloop-like structure (Zwieb, 1992b); several such motifs can be found in the 5S rRNA (Figure 6). We were unable to identify obvious sequence similarities between SRP19 and the three proteins that naturally associate with *E. coli* 5S rRNA (ribosomal proteins L5, L18, and L25) (Garrett & Noller, 1979), with the possible exception of a predominantly basic region located at the N-terminus of ribosomal protein L18.

We have defined the structural and functional potential of the SRP19−SRP RNA complex. A more detailed understanding of the role of protein SRP19 in SRP assembly and function will require information at a higher resolution.

The ability to obtain milligram amounts of highly purified SRP19 protein for biophysical studies such as X-ray crystallography and NMR, will allow us to initiate experiments directed to this goal.

## ACKNOWLEDGMENT

We thank Kimberley Chittenden for excellent technical assistance and Ray Brown for helpful advice on protein purification.

## REFERENCES

Althoff, S., Selinger, D., & Wise, J. (1994) *Nucleic Acids Res. 22*, 1933−1947.
Boehm, S. (1987) *FEBS Lett. 212*, 15−20.
Bradford, M. (1976) *Anal. Biochem. 72*, 248−254.
Chittenden, K., Black, S. D., & Zwieb, C. (1994) *J. Biol. Chem. 269*, 20497−20502.
Christensen, A., Mathiesen, M., Peattie, D., & Garrett, R. (1985) *Biochemistry 24*, 2284−2291.
Douthwaite, S., & Garrett, R. (1981) *Biochemistry 20*, 7301−7307.
Erdmann, V., Wolters, J., Huysmans, E., & De Wachter, R. (1985) *Nucleic Acids Res. 13*, r105−r153.
Fox, G., & Woese, C. (1975) *Nature 256*, 505−507.
Garrett, R., & Noller, H. (1979) *J. Mol. Biol. 132*, 637−648.
Gast, F., & Hagerman, P. (1991) *Biochemistry 30*, 4268−4277.
Gast, F., Amiri, K., & Hagerman, P. (1994) *Biochemistry 33*, 1788−1796.
Gundelfinger, E. D., Krause, E., Melli, M., & Dobberstein, B. (1983) *Nucleic Acids Res. 11*, 7363−7374.
Gutell, R., Weiser, B., Woese, C., & Noller, H. (1985) *Prog. Nucleic Acid Res. Mol. Biol. 32*, 155−216.
Hann, B., Stirling, C., & Walter, P. (1992) *Nature 356*, 532−533.
Krieg, U., Walter, P., & Johnson, A. (1986) *Proc. Natl. Acad. Sci. U.S.A. 83*, 8604−8608.
Kurzchalia, T., Wiedman, M., Girshovich, A., Bochkareva, E., Bielka, H., & Rapoport, T. (1986) *Nature 320*, 634−636.
Larsen, N., & Zwieb, C. (1991) *Nucleic Acids Res. 19*, 209−215.
Lingelbach, K., Zwieb, C., Webb, J. R., Marshallsay, C., Hoben, P. J., Walter, P., & Dobberstein, B. (1988) *Nucleic Acids Res. 16*, 9431−9442.
Maniatis, T., Fritsch, E., & Sambrook, J. (1982) Cold Spring Harbor Laboratory, Cold Spring Harbor, NY.
Miller, J., Wilhelm, H., Gierasch, L., Gilmore, R., & Walter, P. (1993) *Nature 366*, 351−354.
Raner, K. (1993) *Information about MCF is available by E-mail from kraner@acslink.net.au.*
Rasband, W. (1994) *The Image program is in the public domain and available by Anonymous FTP from zippy.nimh.nih.gov.*
Ribes, V., Römisch, K., Giner, A., Dobberstein, B., & Tollervey, D. (1990) *Cell 63*, 591−600.
Römisch, K., Webb, J., Lingelbach, K., Gausepohl, H., & Dobberstein, B. (1990) *J. Cell Biol. 111*, 1793−1802.
Samuelsson, T. (1992) *Nucleic Acids Res. 20*, 5763−5770.
Selinger, D., Brennwald, P., Althoff, S., Reich, C., Hann, B., Walter, P., & Wise, J. (1994) *Nucleic Acids Res. 22*, 2557−2567.
Studier, F. W., Rosenberg, A. H., Dunn, J. J., & Dubendorff, J. W. (1990) *Methods Enzymol. 185*, 60−89.
Tang, R., & Draper, D. (1994) *Biochemistry 33*, 10089−10093.
Walter, P., & Blobel, G. (1983) *Cell 34*, 525−533.
Walter, P., & Lingappa, V. R. (1986) *Annu. Rev. Cell Biol. 2*, 499−516.
Walter, P., Gilmore, R., & Blobel, G. (1984) *Cell 38*, 5−8.
Wiedmann, B., Sakai, H., Davis, T., & Wiedmann, M. (1994) *Nature 370*, 434−440.
Woese, C. R., Winker, S., & Gutell, R. R. (1990) *Proc. Natl. Acad. Sci. U.S.A. 87*, 8467−8471.
Wolffe, A. (1988) *EMBO J. 7*, 1071−1079.
Wray, W., Boulikas, T., Wray, V. P., & Hancock, R. (1981) *Anal. Biochem. 118*, 197−203.
Wu, H., & Crothers, D. (1986) *Nature 308*, 509−513.
Zopf, D., Bernstein, H. D., Johnson, A. E., & Walter, P. (1990) *EMBO J. 9*, 4511−4517.
Zwieb, C. (1985) *Nucleic Acids Res. 13*, 6105−6124.
Zwieb, C. (1989) *Prog. Nucleic Acid Res. Mol. Biol. 37*, 207−234.
Zwieb, C. (1991a) *Biochem. Cell Biol. 69*, 649−654.
Zwieb, C. (1991b) *Nucleic Acids Res. 19*, 2955−2960.
Zwieb, C. (1992a) *Nucleic Acids Res. 20*, 4397−4400.
Zwieb, C. (1992b) *J. Biol. Chem. 267*, 15650−15656.
Zwieb, C. (1994) *Eur. J. Biochem. 222*, 885−890.
Zwieb, C., & Brimacombe, R. (1980) *Nucleic Acids Res. 8*, 2397−2411.
Zwieb, C., & Ullu, E. (1986) *Nucleic Acids Res. 14*, 4639−4657.
Zwieb, C., & Schüler, D. (1989) *Biochem. and Cell Biol. 67*, 434−442.
Zwieb, C., & Brown, R. S. (1990) *Nucleic Acids Res. 18*, 583−587.
Zwieb, C., & Larsen, N. (1994) *Nucleic Acids Res. 22*, 3483−3487.
Zwieb, C., Kim, J., & Adhya, S. (1989) *Genes Dev. 3*, 606−611.

BI950716K